Pretreatment of printing and dyeing wastewater by Fe/C micro-electrolysis combined with H_2O_2 process

Yan Wang, Xianwei Wu, Ju Yi, Lijun Chen, Tianxiang Lan and Jie Dai

ABSTRACT

A novel iron-carbon (Fe/C) micro-electrolysis combined with H_2O_2 (ICMH) process was proposed to pretreat the printing and dyeing wastewater (PDW), using a micro-electrolysis filling. The effects of H_2O_2 concentration, reaction time, initial pH, and Fe/C dosage on chemical oxygen demand (COD) removal rate of PDW were optimized by response surface methodology (RSM). The maximum COD removal rate was approximately 77.65% after 186 min treatment, when the concentration of H_2O_2, initial pH and the dosage of Fe/C were 8.88 g/L, 1.5 and 837 g/L, respectively. Analysis of variance (ANOVA) showed a high coefficient of determination value ($R^2 = 0.9780$). And H_2O_2 concentration and initial pH were the key factors to improve the treatment effect. UV-Vis spectra indicated that a significant blue shift at 220 nm, attributing that fused aromatic hydrocarbons were degraded effectively. 3D-EEM spectra analysis showed that the water samples of PDW mainly contained three kinds of organic matter: refractory fulvic acid, soluble microbial metabolites and aromatic proteins, and the degradation rate of these was 81.76%, 53.78% and 70.83%, respectively.

Key words | 3D-EEM fluorescence spectra, Fenton, micro-electrolysis, printing and dyeing wastewater, response surface methodology, UV-Vis spectra

Yan Wang
Xianwei Wu
Ju Yi
Lijun Chen
Tianxiang Lan
Jie Dai (corresponding author)
College of Chemistry and Environmental Engineering,
Yangtze University,
Jingzhou, Hubei 434023,
China
E-mail: *cjdxdaijie@163.com*

INTRODUCTION

A large volume of complex and refractory organic wastewater is generated from dyeing, printing and sizing processes with the development of the textile industry in recent years (Gupta *et al.* 2015). Such wastewater not only is characterised by high color, poor biodegradability and biological toxicity, but also threatens the balance of ecology and the safety of human beings (Holkar *et al.* 2016; Sultan 2017). Therefore, the removal of these refractory organic compounds has been of great importance before discharging them into surroundings. Herein various techniques have been applied for the pretreatment of printing and dyeing wastewater (PDW), such as adsorption (Gupta & Suhas 2009), filtration (Abid *et al.* 2012), chemical coagulation (Rodrigues *et al.* 2013), oxidation (Meriç *et al.* 2004), and the anaerobic-aerobic process (Punzi *et al.* 2015). However, any single method mentioned above usually has its own limitations, for example long retention time, high cost, and poor removal. Considering these factors, advanced oxidation processes (AOPs) are good choices for further treatment of wastewater because they generate on site hydroxyl radicals (·OH) with high oxidative capability (Muhammad *et al.* 2008; Paul Guin *et al.* 2017), having attracted more and more attention in wastewater pretreatment (Kestioğlu *et al.* 2005; Alaton & Teksoy 2007; Durante *et al.* 2011; Zhou *et al.* 2011). Furthermore, several combination processes have been demonstrated to achieve a better performance in recent years (Oller *et al.* 2011; Bessegato *et al.* 2016; Bustillo-Lecompte & Mehrvar 2016; Xu *et al.* 2016).

Fenton is considered as the most popular among various AOPs, and has been applied to the remediation of wastewater in the pretreatment unit (Badawy & Ali 2006; Deng 2007; Zhuang *et al.* 2015). Besides, Fe/C micro-electrolysis has been proposed as an attractive alternative for refractory wastewater pretreatment process due to its simple operation, low energy consumption and high efficiency (Li *et al.* 2017). Micro-electrolysis utilizes the potential difference between iron and carbon to form a myriad of microscopic galvanic cells, unlike traditional electrolysis (external electrolysis), which requires an external power supply, so micro-electrolysis is also called internal electrolysis. The electrode reactions are listed as follows (Equations

doi: 10.2166/wst.2018.244

(1) and (2)) (Badawy & Ali 2006):

$$\text{Anode(iron): } Fe(s) - 2e^- \rightarrow Fe^{2+}(aq) \quad (1)$$

$$\text{Cathode(carbon): } 2H^+(\text{aq}) + 2\text{e}^- \rightarrow 2[H] \rightarrow H_2(\text{g}) \quad (2)$$

The reaction of Equation (1) produced ferrous ions (Fe^{2+}) into the water, and then triggered the Fenton reaction by adding H_2O_2 as shown in Equations (3)–(5), which could regenerate Fe^{2+} through the oxidation of H_2O_2 or hydroperoxyl radical ($HO_2^{\cdot}$) (Zhang *et al.* 2013).

$$Fe^{2+} + H_2O_2 + H^+ \rightarrow Fe^{3+} + \cdot OH + H_2O \quad (3)$$

$$Fe^{3+} + H_2O_2 \rightarrow Fe^{2+} + HO_2^{\cdot} + H^+ \quad (4)$$

$$Fe^{3+} + HO_2^{\cdot} \rightarrow Fe^{2+} + O_2 + H^+ \quad (5)$$

Under alkaline conditions, the hydroxide was formed by iron ions and hydroxyl with the effect of coagulation and sedimentation, which can be attracted to the weakly negative charged particles in the solution to form a relatively stable floc (iron) (Ying *et al.* 2012).

Some properties of micro-electrolysis and Fenton are conducive to *in situ* coupling. Zhang *et al.* (2013) identified that pH 3 was suitable for micro-electrolysis. Another research found that the maximum organics removal rate reached by Fenton was under pH 2 (Xu *et al.* 2017). So an acidic reaction environment is necessary for these two processes. Moreover, Van der Zee *et al.* (2003) found that the iron and carbon micro-electric field can accelerate electron transfer, the electric field effect will promote Fenton oxidation. Hai *et al.* (2007) also proposed that a combination of two chemical processes could break through some flaws of an individual chemical treatment.

There are usually two kinds of micro-electrolysis and Fenton combined oxidation methods. One is Fe/C micro-electrolysis (ICM) and Sequential Fenton oxidation, which has been developed to be more mature in the past several years (Lan *et al.* 2012; Zhang *et al.* 2012; Xu *et al.* 2016). However, it has some difficulties in application due to the long process flow and the high cost of construction and operation. Another is ICM coupling with *in situ* Fenton technology. *In situ* coupling technology aggravates iron corrosion and promotes recycling utilization of Fe^{2+} and Fe^{3+} (Equations (1), (4) and (5)) due to the existence of H_2O_2. ICM-Sequential Fenton oxidation only utilizes the residual Fe^{2+} in the effluent of micro-electrolysis to react with H_2O_2 and does not guarantee the supply of Fe^{2+}. Zhang *et al.* (2012) found that over 60% chemical oxygen demand (COD) removal rate was achieved after 90 min of internal micro-electrolysis and then 105 min of Fenton process under the optimal conditions for landfill leachate. In another research, hydrogen peroxide-enhanced ICM was used for pretreatment of landfill leachate with the highest COD removal (74.59%) (Wang *et al.* 2016). These studies have demonstrated that ICM-*in situ* Fenton technology is superior to the former technology in pollutant degradation. Therefore, *in situ* coupling technology becomes a promising research focus in the wastewater treatment field; so far this process has not yet explored involving PDW. It is of practical significance to explore the application of micro-electrolysis and Fenton *in situ* coupling technology in the pretreatment of PDW. In addition, the study sample will use actual wastewater to improve the industrial application possibilities.

Response surface methodology (RSM) is the statistical analysis tool to optimize the experimental design and mathematical modeling (Thirugnanasambandham & Sivakumar 2015). Most studies have been carried out to determine the feasibility and performance of the treatment technologies by RSM (Li *et al.* 2010; Gengec *et al.* 2012). UV-Vis spectroscopy and three-dimensional excitation-emission matrix (3D-EEM) fluorescence spectra can identify the types of organic pollutants to look forward to providing a direction for subsequent processing from a biochemical perspective (Sun *et al.* 2016). 3D-EEM spectra is widely used in research into dissolved organic matter (DOM) in water due to its low cost, simple pretreatment, no damage to samples and high sensitivity (Hao *et al.* 2012). Nakamura *et al.* (2009) has reported on the dye analysis of Shosoin textiles by EEM fluorescence and UV-Vis spectrometry.

In this study, a novel micro-electrolysis filling which is easy to clean and produces less iron sludge was used to establish the ICM system. The pretreatment of the actual PDW was investigated by Fe/C micro-electrolysis coupled with the H_2O_2 (ICMH) process without the addition of Fe^{2+}. The effects of H_2O_2 concentration, initial pH, Fe/C dosage and reaction time on the COD removal rate of the actual PDW were investigated by RSM to determine optimal parameters and the higher treatment effect. The degradation mechanism of organic matter in PDW was analyzed by UV-Vis spectroscopy and 3D-EEM spectra.

MATERIALS AND METHODS

Experimental materials

The raw PDW employed in this work was obtained from a comprehensive PDW treatment plant in Jingzhou, China.

The main characteristics of the wastewater were as follows: the initial pH of PDW was in a range of 7.1–7.7 with a high strength of COD_{Cr} (1,000–1,300 mg/L), color (700–800 times), and total salt (3,000–3,400 mg/L).

A commercial micro-electrolysis filling with iron and carbon mass ratio of 1: 1 and spherical particle structure from Beijing Wei Hua Di Ke Technology Co., Ltd was used in this study. This filling was mainly composed of iron and carbon and other catalytic elements with a particle size of 10–14 mm and a specific surface area of 1.2 m^2/g; its porosity and physical strength were 65% and 1,100 kg/cm^2, respectively. The fillings were immersed in the wastewater overnight before being used to eliminate the effect of adsorption, and stored in a beaker containing dilute sulfuric acid to prevent the oxidation of air and promote regeneration after using. Hydrogen peroxide (H_2O_2, 30%, w/v) and other chemicals were of analytical grade.

Experimental procedure

The schematic diagram of the ICMH process is shown in Figure 1, mainly consisting of an air pump (LP-40), flow meters (LZB-10), sour type burette, iron-carbon fillings, contact reactor and other components. The reactor was made from Plexiglas material with dimensions of 17 cm × 10 cm × 30 cm. The initial pH of wastewater was adjusted to the desired values by 0.1 mol/L H_2SO_4 or 0.1 mol/L NaOH solution. The PDW with a total volume of 2 L was poured into the reactor. The appropriate amount of iron-carbon fillings were placed on the bottom plate of the reactor with a height range of about 5–15 cm. Oxygen was introduced via the air pump through porous tubes located at the bottom of the reactor and the gas flow rate was kept at 500 L/h. H_2O_2 was added dropwise through a sour type burette to control a certain flow rate within 30 min. At certain time intervals, samples were taken from the solution and NaOH was added to increase the pH to 9–10. After settling for 30 min, the supernatant was used for COD analysis. All experiments were performed at room temperature.

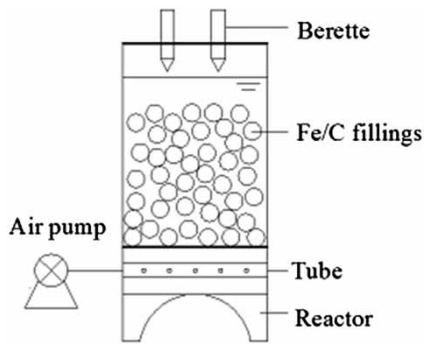

Figure 1 | Schematic of the experiment setup.

Analytical methods

COD was determined by the standard method of potassium dichromate oxidation. Color was measured by the dilution multiple method and values were expressed as x times (0 time indicates that the sample was as clear as pure water). The total salt and pH were analyzed by the weight method and pH meter (PB-10, Sartorius, Germany). Removal rate of COD was calculated as:

$$Removal\ rate\ (\%) = \frac{C_0 - C}{C_0} \quad (6)$$

where C_0 and C are the initial and residual COD in wastewater.

The absorbance of samples was further analyzed by a UV-2450 UV-Vis spectrophotometer (Shimadzu, Japan) with a wavelength range of 190–600 nm. The 3D-EEM fluorescence spectra were obtained using a LS-55 fluorescence spectrophotometer (Perkin-Elmer, USA). Excitation (Ex) wavelengths were conducted from 200 to 500 nm at 10 nm intervals and emission (Em) wavelengths were conducted every 0.5 nm from 280 to 550 nm with a scanning speed of 1,200 nm/min. Slit widths of Ex and Em were both set at 5 nm. Before measurements, the samples were filtrated with a 0.45 μm CA membrane filter and diluted with Milli-Q ultrapure water to an optical density.

Experimental design

Before the experimental design, preliminary experiments were carried out for different variables and their ranges. In order to evaluate the influence of operating parameters, the removal rate of COD (Y) of PDW was investigated by the Box-Behnken Design (BBD) of Design Expert 8.0 software. Four main variables were chosen: H_2O_2 concentration (A), reaction time (B), initial pH (C) and Fe/C dosage (D). The ranges and levels of experimental variables are listed in Table 1. The total number of experiments conducted was 29, including five groups of centre replications

Table 1 | The ranges and levels of experimental variables

Variables	Symbol	Range and levels		
		−1	0	+1
H_2O_2 concentration (g/L)	A	6.66	8.88	11.1
Reaction time (min)	B	120	180	240
Initial pH	C	1.5	3	4.5
Fe/C dosage (g/L)	D	400	800	1,200

to assess the pure error. Experimental design and results are presented in Table 2.

Table 2 | Experimental design and results

Run	(A) H_2O_2 concentration (g/L)	(B) Reaction time (min)	(C) Initial pH	(D) Fe/C dosage (g/L)	(Y_1) COD removal rate (%)
1	11.1	180	3	400	45.84
2	8.88	240	3	400	57.48
3	8.88	180	1.5	1,200	71.04
4	8.88	180	3	800	72.38
5	8.88	180	1.5	400	73.46
6	8.88	180	4.5	400	43.27
7	8.88	120	4.5	800	46.19
8	6.66	180	4.5	800	45.76
9	6.66	180	1.5	800	71.25
10	8.88	180	3	800	69.72
11	8.88	120	3	400	56.49
12	8.88	120	1.5	800	69.84
13	11.1	240	3	800	54.65
14	8.88	180	3	800	68.29
15	8.88	240	4.5	800	48.57
16	8.88	240	1.5	800	72.85
17	11.1	180	4.5	800	37.18
18	8.88	180	3	800	72.18
19	8.88	120	3	1,200	64.93
20	6.66	180	3	1,200	63.84
21	6.66	120	3	800	60.94
22	8.88	180	3	800	70.42
23	8.88	180	4.5	1,200	49.71
24	11.1	180	3	1,200	52.36
25	11.1	120	3	800	52.61
26	8.88	240	3	1,200	63.84
27	6.66	240	3	800	62.43
28	11.1	180	1.5	800	64.89
29	6.66	180	3	400	50.97

The experiment data were obtained under designed conditions and analyzed by the response surface regression procedure to fit a model. Performance was evaluated by analyzing the COD removal rate, as shown in Table 3. The results were explained through an empirical second-order quadratic polynomial Equation (7) (Güven *et al.* 2009).

$$Y = \beta_0 + \sum_{i=1}^{k} \beta_i X_i + \sum_{i=1}^{k} \beta_{ii} X_i^2 + \sum_{i=1}^{k-1} \sum_{j=2}^{k} \beta_{ij} X_i X_j + \varepsilon \quad (7)$$

where Y is the predicted response, β_0, β_i, β_{ii}, β_{ij} is the set of regression coefficients, ε is the random error value, X_i, X_j are coded variables.

The quality of the polynomial fit model equation was evaluated by the coefficient of regression (R^2), adjusted R^2, coefficient of variation (CV), adequate precision (AP), and its statistical significance was checked by Fisher's F-test. The analysis of variance (ANOVA) was needed to test the significance and adequacy of the model. Three-dimensional surface plots were obtained to evaluate individual and interactive effect of variables on the response. The numerical optimization process was utilized to optimize the level of each variable for maximum responses.

Table 3 | Analysis of variance for COD removal rate regression equation

Source	Sum of squares	df	Mean square	F-value	p-value Prob > F
Model	3,150.11	14	225.01	44.48	<0.0001
A	189.29	1	189.29	37.42	<0.0001
B	6.48	1	6.48	1.28	0.2767
C	1,941.84	1	1,941.84	383.82	<0.0001
D	121.67	1	121.67	24.05	0.0002
AB	0.076	1	0.076	0.015	0.9044
AC	1.23	1	1.23	0.24	0.6293
AD	10.08	1	10.08	1.99	0.1799
BC	0.099	1	0.099	0.020	0.8906
BD	1.08	1	1.08	0.21	0.6509
CD	19.62	1	19.62	3.88	0.0690
A^2	645.44	1	645.44	127.58	<0.0001
B^2	101.86	1	101.86	20.13	0.0005
C^2	238.52	1	238.52	47.15	<0.0001
D^2	246.25	1	246.25	48.67	<0.0001
Residual	70.83	14	5.06		
Lack of fit	59.02	10	5.90	2.00	0.2633
Pure error	11.81	4	2.95		
Cor total	3,220.93	28			

$R^2 = 0.9780$, adjusted $R^2 = 0.9560$, AP = 22.794, CV% = 3.76.

RESULTS AND DISCUSSION

A comparative study

In order to evaluate the effect of ICM and Fenton oxidation, the comparative tests were conducted under adding H_2O_2 or not with the conditions of pH 3, Fe/C dosage of 800 g/L and an aeration rate of 500 L/h for 90 min. The results showed that the removal rate of COD for ICM was 48.31%, the COD removal rate of ICMH increased by 20%. The treatment efficiency of ICMH was significantly higher than ICM, which may be related to micro-electrolysis and Fenton co-oxidation. Fe^{2+} generated by micro-electrolysis was used to accelerate the Fenton chain reaction to produce strong oxidation ·OH, leading to the effective degradation of organics. It can be demonstrated that the ICMH process of PDW pretreatment has better performance.

Model statistical analysis for ICMH

Under different conditions, the COD removal rate varied from 37.18% to 73.46%. The second-order quadratic polynomial regression equation model established with the response values (Y_1) can be expressed as Equation (8):

$$Y_1 = 70.60 - 3.97A + 0.74B - 12.72C + 3.18D + 0.18AB - 0.55AC - 1.59AD - 0.16BC - 0.52BD + 2.21CD - 9.98A^2 - 3.96B^2 - 6.06C^2 - 6.16D^2 \quad (8)$$

Model terms were evaluated by the P value with 95% confidence levels. According to the ANOVA (Table 3), the F-statistics value was higher, and its value was 44.48 for COD. The large F-value indicated that most of the variation in the response could be explained by the regression model. The model is significant when Prob > F value is less than 0.05, the value of Prob > F less than 0.0001 indicates that the term is highly significant (Orbahti *et al.* 2007). In this study, the value of Prob > F was less than 0.0001 for the model. Among all the independent variables, initial pH had a large effect on the COD removal ($P < 0.0001$).

R^2 and Adj-R^2 were significant parameters in the model. They showed adequate variation of the quadratic model to the experimental data. In this research, the R^2 value for COD removal was at 0.9780. This means 97.80% of the variation for COD removal rate was explained by the independent variables and only 2.2% of variation of the model is not explained. The Adj-R^2 was at 0.9560 for COD removal. The CV is the value of the reproducibility of the model and should be lower than 10% (Gengec *et al.* 2012). Therefore the CV of 3.76% demonstrated the reliability and high precision of the experimental data. The AP illustrates the range of the predicted data of the average prediction error. AP measures the signal to noise ratio, and its value of more than 4 is desirable (Güven *et al.* 2009). Thus, the quadratic model can be applied to navigate the BBD design. The AP ratio of the models in this study was 22.794, which was greater than 4, indicating that the response was adequate.

Response surface for ICMH process

Figure 2 shows the three-dimensional surface plots of the COD removal over the independent variables. Figure 2(a) depicts the percentage of the COD removal rate as a function of the H_2O_2 concentration and reaction time while keeping the initial pH and Fe/C dosage at constant values of 3 and 800 g/L, respectively. It can be seen that changes in the reaction time had little impact on the COD removal rate. With the increase of H_2O_2 concentration, the COD removal rate had a lot of volatility, which increased to a point (72.38%) and then decreased. This may be related to a large number of ·OH with high reactivity generated in the coupling process. After the H_2O_2 concentration reached a certain level, excessive H_2O_2 could convert into HO_2, as in the following Equation (4), which exhibited such a lower oxidation power than ·OH. What was more, the production of ·OH was in turn reduced sharply.

Figure 2(b) illustrates the effect of the H_2O_2 concentration and initial pH on removal rate for reaction time and Fe/C dosage of 180 min and 800 g/L, respectively. The COD removal rate increased sharply in the pH range 1.5–2.5 and slightly changed at pH above 3. Enough supplement of H^+ seems to favor the occurrence of Equation (3). This was related to the relatively large difference of Fe/C potential at acidic level, which was convenient to accelerate electron transfer, assisting Fenton reactions in the micro-electric field. When the initial pH rose to 4.5, the precipitation of both Fe^{2+} and Fe^{3+} blocks the electron transfer between the iron and the PDW. Moreover, the regeneration of Fe^{2+} via Equation (4) was slow. Consequently, less H_2O_2 was produced, leading to reduction in the rate of oxidation reaction.

Figure 2(c) shows the response surface plots of the removal rate as a function of the H_2O_2 concentration and Fe/C dosage at the reaction time and initial pH of 180 min and 3, respectively. The removal increased with both increasing H_2O_2 concentration and Fe/C dosage (up to the

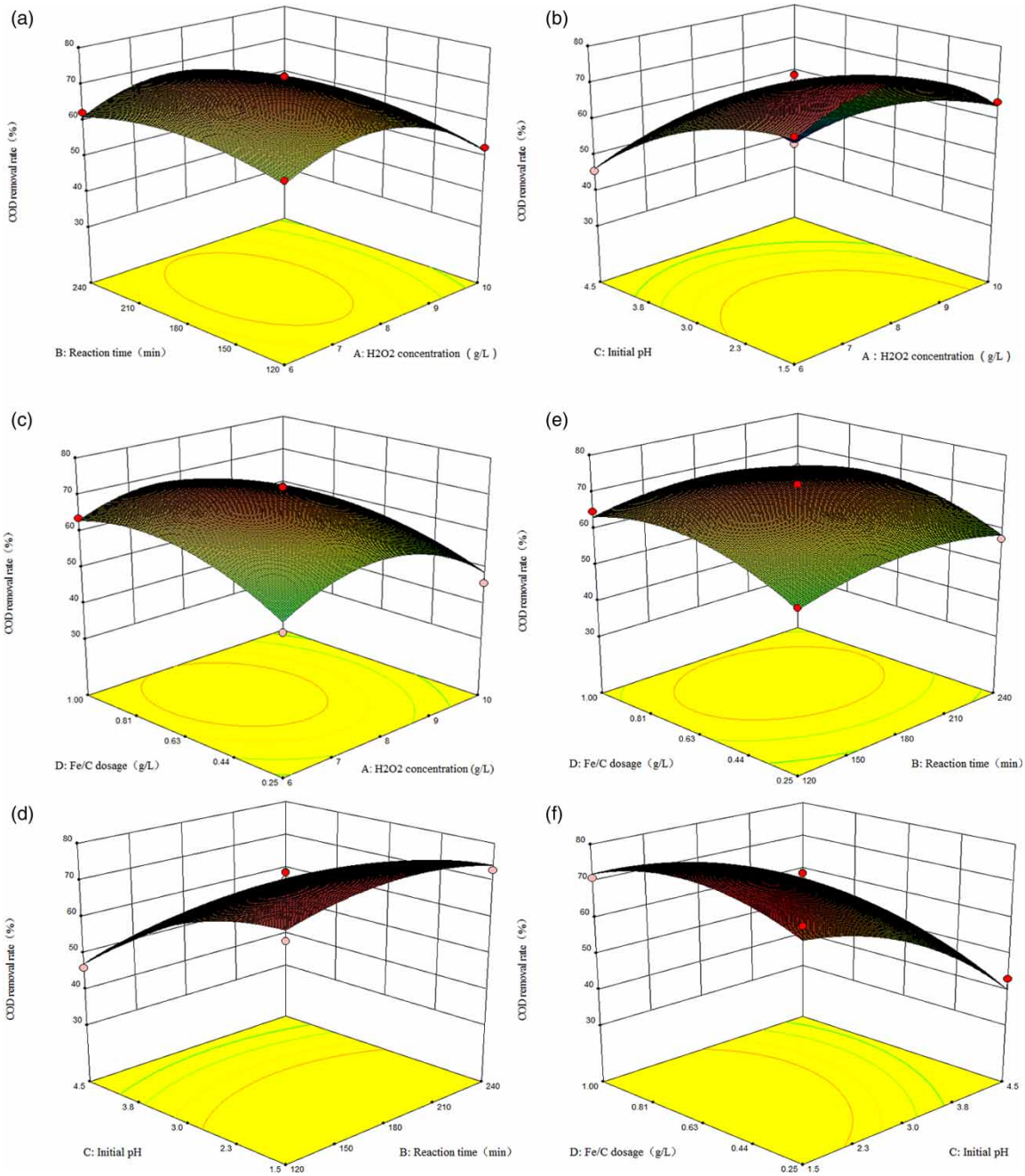

Figure 2 | The three-dimensional surface plots of the COD removal rate as a function of: (a) H_2O_2 concentration and reaction time at fixed initial pH (3) and Fe/C dosage (800 g/L), (b) H_2O_2 concentration and initial pH with reaction time and Fe/C dosage at their middle levels, (c) H_2O_2 concentration and Fe/C dosage at fixed reaction time (180 min) and initial pH (3), (d) reaction time and initial pH with H_2O_2 concentration and Fe/C dosage at their middle levels, (e) reaction time and Fe/C dosage at fixed H_2O_2 concentration (8.88 g/L) and initial pH (3), (f) initial pH and Fe/C dosage with H_2O_2 concentration and reaction time at their middle levels.

middle level). Also, it can be seen that Fe/C dosage had little effect on the COD removal rate in the beginning due to the number of galvanic cells. When the Fe/C dosage was 400 g/L, the micro-electrolysis reaction was inhibited by the lack of Fe^{2+}, resulting in lower ·OH production. This phenomenon was improved when the Fe/C fillings dosage was 800 g/L. The contact area between the Fe/C fillings and wastewater increased with the increase in Fe/C dosage; a large number of galvanic cells could promote the oxidation of Fe to Fe^{2+} to redox reaction (Equation (3)) in different reactive sites, which contributes to the mineralization of organic pollutants. However, the excess Fe^{2+},

Fe^{3+} floc formed had a bad sedimentation property and the process was slow, leading to poor COD removal.

Figure 2(d) illustrates the interactive effect of the initial pH and reaction time on the removal rate at the H_2O_2 concentration of 8.88 g/L and Fe/C dosage of 800 g/L, respectively. COD removal increased with reaction time. More and more ·OH were produced by [H] and Fe^{2+} catalytic reaction with H_2O_2, which promoted the oxidative degradation of organic pollutants in water to a certain extent. However, when the reaction was carried out for a period of time, the removal decreased with increasing reaction time after a time of 186 min for COD removal. This was due to the large amount of H_2O_2 production, which causes H_2O_2 to break down into oxygen and water. With increasing reaction time, Fe was easily oxidized to form Fe^{3+} oxide film, the Fe/C micro-electrolysis filling was blunted owing to the prolonged presence of Fe in aerobic conditions, hindering the progress of the redox reaction (Cheng *et al.* 2007).

Percentage of removal rate for H_2O_2 concentration and initial pH of 8.88 g/L and 3 obtained as a function of reaction time and Fe/C dosage is depicted in Figure 2(e). The COD removal rate was 50.97% when the reaction time and Fe/C dosage were both kept at their lowest studied level. And these have improved by 21.41% through increasing reaction time and Fe/C dosage. The effect of interaction between initial pH and Fe/C dosage on removal rate is presented in the response surface plot of Figure 2(f) for H_2O_2 concentration and a reaction time of 8.88 g/L and 180 min, respectively. It was obvious that higher COD removal could be reached under a strong acid environment and large Fe/C dosage. Based on the above discussion, the main variable of this process that improved the COD and color removal were H_2O_2 concentration and initial pH.

Optimization results

Variable parameters were optimized for optimal removal by Design Expert 8.0, the response (COD removal rate) were defined as 'maximum' to achieve the better performance among variable parameters. The result indicated that 77.65% COD removal rate were obtained when the H_2O_2 concentration of 8.88 g/L, the reaction time of 186 min, the initial pH of 1.5, the dosage of Fe/C of 837 g/L. In theory, the COD concentration can be reduced to 300–400 mg/L.

To confirm the adequacy of the model, an additional experiment under optimized operational conditions was carried out which was revealing agreement with the predicted responses. It implies that the way to optimize COD removal rate by RSM for the PDW with ICMH process was successful.

CHANGES IN ORGANIC MATTER

UV-Vis spectral analysis

UV-Vis spectral changes of PDW during reaction in the ICMH process under optimization condition are displayed in Figure 3. Before treatment, the UV-Vis spectrum of PDW exhibited a main absorption band in the UV region (<300 nm). However, as soon as the activated reaction started, the intensity of the UV band obviously decreased and the peak area decreased greatly. This showed that ICMH has an observable effect on the degradation of PDW. The strong absorption peak of the raw water sample at 200 nm to 260 nm indicated that there are heterocyclic unsaturated systems, benzene rings and conjugated double bonds in the organic matter (Kusic *et al.* 2009). Because the wastewater of this study used was a mixed PDW, it was impossible to determine the specific dye type. UV_{254} is an important control parameter for measuring organic indices in water (Uyguner & Bekbolet 2005). The peak at 254 nm decreased step by step, indicating that the macromolecular organic compounds in water gradually degraded into small organic molecules. Meanwhile, the absorption band at 220 nm appeared a significant blue shift phenomenon, which may be caused by the decrease of aromatic hydrocarbons and the conjugate structure.

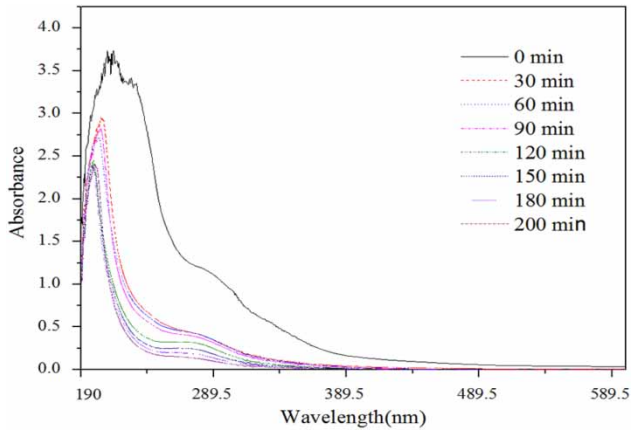

Figure 3 | UV-vis spectra of pretreatment of PDW as a function of time with H_2O_2 concentration of 8.88 g/L, a reaction time of 186 min, an initial pH of 1.5, and a dosage of Fe/C of 837 g/L.

Moreover, water samples had correspondingly no spectral bands in the VIS region for 200 min. On the other side, spectral bands in the UV region were still present, indicating the incomplete mineralization of organics in wastewaters.

Three-dimensional fluorescence spectroscopy

Eextra experiments were carried out using the optimization parameters obtained. The behavior of DOM in wastewater is illustrated by 3D-EEM spectra in Figure 4. There were

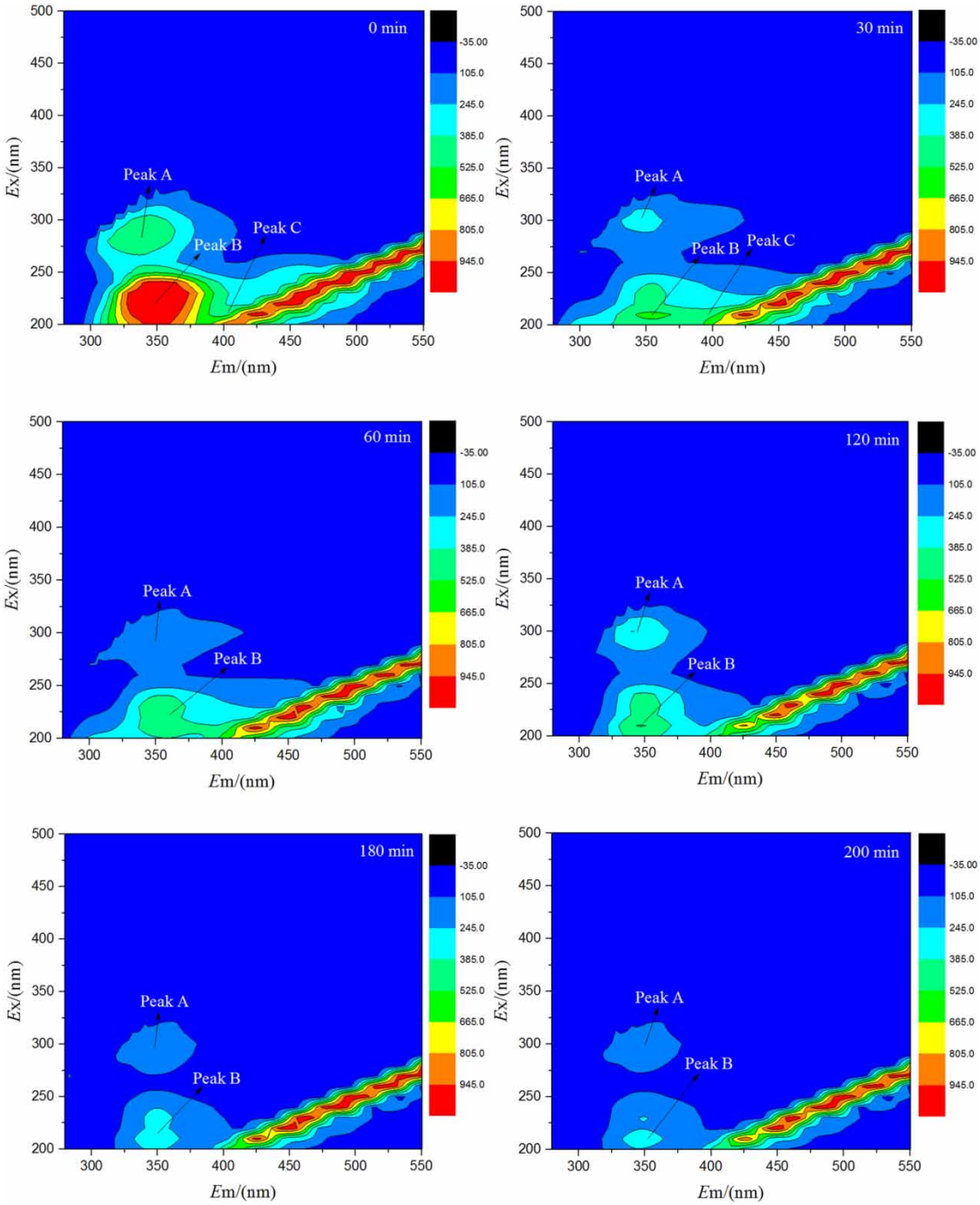

Figure 4 | 3D-EEM spectra of pretreatment of PDW as a function of time with H_2O_2 concentration of 8.88 g/L, the reaction time of 186 min, the initial pH of 1.5, the dosage of Fe/C of 837 g/L.

three typical fluorescence peaks: soluble microbial products peak A: $\lambda_{Ex}/\lambda_{Em}$ = (240–300/310–360) nm; tryptophane-like aromatic protein peak B: $\lambda_{Ex}/\lambda_{Em}$ = (200–240/320–370) nm; and fulvic-like substances peak C: $\lambda_{Ex}/\lambda_{Em}$ = (220–250/380–450) nm (Chen *et al.* 2003). It was reported that soluble microbial products and tryptophane-like aromatic protein were suitable for biodegradation (Liu *et al.* 2015), although with a fluorescence intensity greater than 500 au and 1,000 au, respectively. In addition, fulvic-like substances with a fluorescence intensity of about 800 au have attracted attention in the pretreatment of PDW.

In the 3D-EEM spectra of effluent from different reaction times, there was an obvious difference in fluorescence intensity and fluorescent region after pretreatment, indicating that this process was feasible. The result indicated that this process not only greatly reduced the content of organic compounds, but also a refractory fulvic-like substances had a better treatment with the degradation rate of 81.76%. The structure and functional groups of the organic substance effectively has been destroyed by synergistic oxidation. The degradation rates of Peak A and Peak B were 53.78% and 70.83%, respectively. Although they were degradable, the fluorescence intensity changed slowly, it may be that fulvic-like substances were continuously degraded into soluble microbial products and tryptophane-like aromatic protein during the reaction. Figure 4 (200 min) shows that DOM is mainly ascribed to soluble microbial products and tryptophane-like aromatic protein, which were suitable to biological treatment, so ICMH process could reach the target for the pretreatment of PDW, which reduced the toxicity and loading shock of the subsequent biochemical treatment units.

CONCLUSION

1. The pretreatment of PDW by ICMH was investigated by RSM. The results showed that H_2O_2 dosage and initial pH were the key factors affecting the efficiency of the treatment. 77.65% COD removal rate was obtained with a H_2O_2 concentration of 8.88 g/L, a reaction time of 186 min, ab initial pH of 1.5, the dosage of Fe/C of 837 g/L. The second-order quadratic model based on the results can better reflect the effect of each variable on the treatment effect.
2. Both UV-Vis spectra and 3D-EEM spectra showed that the pretreatment of PDW by ICMH had an obvious effect. Most macromolecular organic compounds were transformed into small molecules and their biodegradability is enhanced. The UV-Vis spectra of the absorption band at 220 nm showed a significant blue shift, indicating that the condensed ring aromatic hydrocarbons were degraded into small molecules; 3D-EEM spectra showed that the PDW contain three main types of organic matter, including refractory fulvic-like substances, soluble microbial products and tryptophane-like aromatic protein with degradation rates of 81.76%, 53.78% and 70.83%, respectively.

ACKNOWLEDGEMENTS

This work was financially supported by the National Natural Science Foundation of China (No. 21173026).

REFERENCES

Abid, M. F., Zablouk, M. A. & Abid-Alameer, A. M. 2012 Experimental study of dye removal from industrial wastewater by membrane technologies of reverse osmosis and nanofiltration. *Iranian J. Environ. Health Sci. Eng.* **9** (1), 17.

Alaton, I. A. & Teksoy, S. 2007 Acid dyebath effluent pretreatment using Fenton's reagent: process optimization, reaction kinetics and effects on acute toxicity. *Dyes Pigments* **73** (1), 31–39.

Badawy, M. I. & Ali, M. E. M. 2006 Fenton's peroxidation and coagulation processes for the treatment of combined industrial and domestic wastewater. *J. Hazard. Mater.* **136** (3), 961–966.

Bessegato, G. G., Cardoso, J. C., Da Silva, B. F. & Zanoni, M. V. B. 2016 Combination of photoelectrocatalysis and ozonation: a novel and powerful approach applied in Acid Yellow 1 mineralization. *Appl. Catal. B-Environ.* **180**, 161–168.

Bustillo-Lecompte, C. F. & Mehrvar, M. 2016 Treatment of an actual slaughterhouse wastewater by integration of biological and advanced oxidation processes: modeling, optimization, and cost-effectiveness analysis. *J. Environ. Manage.* **182**, 651–666.

Chen, W., Westerhoff, P., Leenheer, J. A. & Booksh, K. 2003 Fluorescence excitation-emission matrix regional integration to quantify spectra for dissolved organic matter. *Environ. Sci. Technol.* **37** (24), 5701–5710.

Cheng, H., Xu, W., Liu, J., Wang, H., He, Y. & Chen, G. 2007 Pretreatment of wastewater from triazine manufacturing by coagulation, electrolysis, and internal microelectrolysis. *J. Hazard. Mater.* **146** (1–2), 385–392.

Deng, Y. 2007 Physical and oxidative removal of organics during Fenton treatment of mature municipal landfill leachate. *J. Hazard. Mater.* **146** (1–2), 334–340.

Durante, C., Cuscov, M., Isse, A. A., Sandonà, G. & Gennaro, A. 2011 Advanced oxidation processes coupled with electrocoagulation for the exhaustive abatement of Cr-EDTA. *Water Res.* **45** (5), 2122–2130.

Gengec, E., Kobya, M., Demirbas, E., Akyol, A. & Oktor, K. 2012 Optimization of baker's yeast wastewater using response surface methodology by electrocoagulation. *Desalination* **286**, 200–209.

Gupta, V. K. & Suhas 2009 Application of low-cost adsorbents for dye removal–A review. *J. Environ. Manage.* **90**, 2313–2342.

Gupta, V. K., Khamparia, S., Tyagi, I., Jaspal, D. & Malviya, A. 2015 Decolorization of mixture of dyes: a critical review. *Global J. Environ. Sci. Manage.* **1**, 71–94.

Güven, G., Perendeci, A. & Tanyolac, A. 2009 Electrochemical treatment of simulated beet sugar factory wastewater. *Chem. Eng. J.* **151**, 149–159.

Hai, F. I., Yamamoto, K. & Fukushi, K. 2007 Hybrid treatment systems for dye wastewater. *Crit. Rev. Environ. Sci. Technol.* **37** (4), 315–377.

Hao, R., Ren, H., Li, J., Ma, Z., Wan, H., Zheng, X. & Cheng, S. 2012 Use of three-dimensional excitation and emission matrix fluorescence spectroscopy for predicting the disinfection by-product formation potential of reclaimed water. *Water Res.* **46** (17), 5765–5776.

Holkar, C. R., Jadhav, A. J., Pinjari, D. V., Mahamuni, N. M. & Pandit, A. B. 2016 A critical review on textile wastewater treatments: possible approaches. *J. Environ. Manage.* **182**, 351–366.

Kestioğlu, K., Yonar, T. & Azbar, N. 2005 Feasibility of physico-chemical treatment and Advanced Oxidation Processes (AOPs) as a means of pretreatment of olive mill effluent (OME). *Process Biochem.* **40** (7), 2409–2416.

Kusic, H., Koprivanac, N., Horvat, S., Bakija, S. & Bozic, A. L. 2009 Modeling dye degradation kinetic using dark- and photo-Fenton type processes. *Chem. Eng. J.* **155** (1–2), 144–154.

Lan, S., Ju, F. & Wu, X. 2012 Treatment of wastewater containing EDTA-Cu(II) using the combined process of interior microelectrolysis and Fenton oxidation-coagulation. *Sep. Purif. Technol.* **89**, 117–124.

Li, M., Feng, C., Zhang, Z., Chen, R., Xue, Q., Gao, C. & Sugiura, N. 2010 Optimization of process parameters for electrochemical nitrate removal using Box-Behnken design. *Electrochim. Acta* **56** (1), 265–270.

Li, P., Liu, Z., Wang, X., Guo, Y. & Wang, L. 2017 Enhanced decolorization of methyl orange in aqueous solution using iron–carbon micro-electrolysis activation of sodium persulfate. *Chemosphere* **180**, 100–107.

Liu, Z., Wu, W., Shi, P., Guo, J. & Cheng, J. 2015 Characterization of dissolved organic matter in landfill leachate during the combined treatment process of air stripping, Fenton, SBR and coagulation. *Waste Manage.* **41**, 111–118.

Meriç, S., Kaptan, D. & Ölmez, T. 2004 Color and COD removal from wastewater containing Reactive Black 5 using Fenton's oxidation process. *Chemosphere* **54** (3), 435–441.

Muhammad, A., Shafeeq, A., Butt, M. A., Rizvi, Z. H., Chughtai, M. A. & Rehman, S. 2008 Decolorization and removal of COD and BOD from raw and biotreated textile dye bath effluent through advanced oxidation processes (AOPS). *Braz. J. Chem. Eng.* **25**, 453–459.

Nakamura, R., Tanaka, Y., Ogata, A. & Naruse, M. 2009 Dye analysis of shosoin textiles using excitation-emission matrix fluorescence and ultraviolet-visible reflectance spectroscopic techniques. *Anal. Chem.* **81** (14), 5691–5698.

Oller, I., Malato, S. & Sánchez-Pérez, J. A. 2011 Combination of advanced oxidation processes and biological treatments for wastewater decontamination-A review. *Sci. Total Environ.* **409** (20), 4141–4166.

Orbahti, B. K. K., Aktas, N. & Tanyolac, A. 2007 Optimization of electrochemical treatment of industrial paint wastewater with response surface methodology. *J. Hazard. Mater.* **148**, 83–90.

Paul Guin, J., Bhardwaj, Y. K. & Varshney, L. 2017 Mineralization and biodegradability enhancement of Methyl Orange dye by an effective advanced oxidation process. *Appl. Radiat. Isotopes* **122**, 153–157.

Punzi, M., Nilsson, F., Anbalagan, A., Svensson, B., Jönsson, K., Mattiasson, B. & Jonstrup, M. 2015 Combined anaerobic–ozonation process for treatment of textile wastewater: removal of acute toxicity and mutagenicity. *J. Hazard. Mater.* **292**, 52–60.

Rodrigues, C. S. D., Madeira, L. M. & Boaventura, R. A. R. 2013 Treatment of textile dye wastewaters using ferrous sulphate in a chemical coagulation/flocculation process. *Environ. Technol.* **34** (6), 719–729.

Sultan, M. 2017 Polyurethane for removal of organic dyes from textile wastewater. *Environ. Chem. Lett.* **15** (2), 347–366.

Sun, M., Wu, M., Liu, W., Liu, H., Zhang, Y. & Dai, J. 2016 3DEEM spectroscopy analysis to assess the EPS composition in different carriers in HMBR systems. *Water Sci. Technol.* **74**, 2708–2716.

Thirugnanasambandham, K. & Sivakumar, V. 2015 Optimization of treatment of grey wastewater using Electro-Fenton technique – modeling and validation. *Process Saf. Environ.* **95**, 60–68.

Uyguner, C. S. & Bekbolet, M. 2005 Evaluation of humic acid photocatalytic degradation by UV–vis and fluorescence spectroscopy. *Catal. Today* **101** (3–4), 267–274.

Van der Zee, F. P., Bisschops, I. A. E., Lettinga, G. & Field, J. A. 2003 Activated carbon as an electron acceptor and redox mediator during the anaerobic biotransformation of azo dyes. *Environ. Sci. Technol.* **37** (2), 402–408.

Wang, L., Yang, Q., Wang, D., Li, X., Zeng, G., Li, Z., Deng, Y., Liu, J. & Yi, K. 2016 Advanced landfill leachate treatment using iron-carbon microelectrolysis-Fenton process: process optimization and column experiments. *J. Hazard. Mater.* **318**, 460–467.

Xu, X., Cheng, Y., Zhang, T., Ji, F. & Xu, X. 2016 Treatment of pharmaceutical wastewater using interior micro-electrolysis/Fenton oxidation-coagulation and biological degradation. *Chemosphere* **152**, 23–30.

Xu, J., Long, Y., Shen, D., Feng, H. & Chen, T. 2017 Optimization of Fenton treatment process for degradation of refractory organics in pre-coagulated leachate membrane concentrates. *J. Hazard. Mater.* **323**, 674–680.

Ying, D., Xu, X., Li, K., Wang, Y. & Jia, J. 2012 Design of a novel sequencing batch internal micro-electrolysis reactor for

treating mature landfill leachate. *Chem. Eng. Res. Des.* **90**, 2278–2286.

Zhang, H., Xiang, L., Zhang, D. & Qing, H. 2012 Treatment of landfill leachate by internal microelectrolysis and sequent Fenton process. *Desali. Water Treat.* **47**, 243–248.

Zhang, S., Wang, D., Zhou, L., Zhang, X., Fan, P. & Quan, X. 2013 Intensified internal electrolysis for degradation of methylene blue as model compound induced by a novel hybrid material: multi-walled carbon nanotubes immobilized on zero-valent iron plates (Fe^0-CNTs). *Chem. Eng. J.* **217**, 99–107.

Zhou, T., Lim, T., Chin, S. & Fane, A. G. 2011 Treatment of organics in reverse osmosis concentrate from a municipal wastewater reclamation plant: feasibility test of advanced oxidation processes with/without pretreatment. *Chem. Eng. J.* **166** (3), 932–939.

Zhuang, H., Han, H., Ma, W., Hou, B., Jia, S. & Zhao, Q. 2015 Advanced treatment of biologically pretreated coal gasification wastewater by a novel heterogeneous Fenton oxidation process. *J. Environ. Sci-China* **33**, 12–20.

First received 24 January 2018; accepted in revised form 16 May 2018. Available online 1 June 2018